Molecular Vision 2001; 7:145-53 <http://www.molvis.org/molvis/v7/a21>
Received 3 September 2000 | Accepted 13 May 2001 | Published 27 June 2001

Effect of H-7 on cultured human trabecular meshwork cells

Xuyang Liu,[1] Suping Cai,[1] Adrian Glasser,[1] Tova Volberg,[2] Jon R. Polansky,[3] Donald J. Fauss,[3] Curtis R. Brandt,[1] Benjamin Geiger,[2] Paul L. Kaufman[1]

[1]Department of Ophthalmology & Visual Sciences, University of Wisconsin, Madison, WI; [2]Department of Molecular Cell Biology, Weizmann Institute of Science, Rehovot, Israel; [3]Department of Ophthalmology, University of California at San Francisco, San Francisco, CA

Purpose: To determine the effect of the serine-threonine kinase inhibitor H-7, which blocks actomyosin contractility and increases outflow facility in live monkeys, on morphology, cytoskeleton, and cellular adhesions of human trabecular meshwork (HTM) cells in culture.
Methods: Cultured HTM cells were videographically recorded and evaluated before and after exposure to H-7 at different concentrations. The subcellular distribution of the actin-based cytoskeleton and associated anchor proteins including vinculin, paxillin, and β-catenin, as well as phosphotyrosine-containing proteins were evaluated by fluorescence immunocytochemistry and digital fluorescence microscopy.
Results: H-7 induced pronounced but reversible HTM cell thickening toward the cell center and deterioration of the actin cytoskeletal network. Cell-extracellular matrix (ECM) and cell-cell adhesions were also affected, but the β-catenin-rich, vinculin-containing adherens junctions were clearly more resistant than focal contacts. Phosphotyrosine labeling in focal contacts was highly sensitive to H-7.
Conclusions: H-7 induces alterations in cell shape, actin cytoskeleton, and associated focal adhesions in cultured HTM cells, which may be responsible for the effects of H-7 on outflow facility in live monkey eyes.

Intracameral and topical administration of H-7 (1-(5-isoquinolinyl-sulfonyl)-2-methylpiperazine), a broad-spectrum serine-threonine kinase inhibitor, reversibly increases outflow facility across the trabecular meshwork, and reduces intraocular pressure (IOP), in live monkey eyes [1,2], and thus this drug has potential as an anti-glaucoma agent. To date, the effects of H-7 on the contractility, morphology, and adhesion molecules of cultured cells, including human trabecular meshwork (HTM) cells, have been studied [1,3,4]. In cultured bovine aortic endothelial cells (BAEC), exposure to H-7 results in a reversible disruption of actin microfilaments and a major alteration in the organization of cell-ECM adhesions [1]. In cultured HTM cells, H-7 blocks cellular contraction induced by ethacrynic acid, colchicine, and vinblastine, and disrupts actin filaments of HTM and Schlemm's canal (SC) cells without altering cell-cell contacts [3,4]. However, changes in morphology of living cells and changes in cellular adhesion characteristics of cultured HTM cells, such as measures of vinculin, β-catenin, paxillin, and phosphotyrosine, upon H-7 treatment have not been extensively examined previously. Such information might help to better understand the cellular and molecular basis for H-7's effect on outflow facility in vivo. In the present study, we specifically evaluated the effects of H-7 on morphology of living HTM cells in culture, and on dynamics of cellular adhesions of HTM cells. For the latter, particularly, a novel fluorescence microscopic approach (fluorescence ratio imaging; FRI) was used, and the labeling intensities and dynamics of the adhesion molecules were analyzed. The novel element in this analysis is the combination of image superimposition and FRI [5], which creates a unique immunofluorescent forum for the rapid quantitative investigation of the diversity in the fine distribution of cellular proteins and cellular changes. The unique feature of FRI is that it is highly sensitive to local differences in the relative fluorescent staining intensities irrespective of their absolute intensities, and can provide valuable information for even faintly labeled structures [5]. The HTM cells used in this study were cultured from an undifferentiated stage with fibroblast-like morphology to a highly confluent monolayer showing stable endothelial-like morphology, to resemble and behave as close to the in vivo situation as possible.

This study reports and discusses the effects of H-7 on HTM cells with emphasis on (a) shape changes of living cells, (b) molecular dynamics of cellular adhesions, and (c) comparison with our in vivo studies including H-7 induced changes in outflow facility, TM ultrastructure, and potential side effects of the drug. Most of these issues and relationships have not been addressed in previous studies with H-7.

METHODS

HTM cell culture and H-7 treatment: HTM cells [6] were grown on Petri dishes or glass cover slips pre-coated with poly-L-lysine (Sigma Chemical Co., St. Louis, MO) and maintained in Dulbecco's modified Eagle medium (DMEM) supplemented with 10% fetal bovine serum, 25 µg/ml gentamycin and 2.5 µg/ml amphotericin B, at 37°C, 8% CO_2. Cells of 3rd-5thpassage were cultured to high confluence for 1 week, at which time

Correspondence to: Paul L. Kaufman, M.D., Department of Ophthalmology and Visual Sciences, F4/328 Clinical Science Center, 600 Highland Avenue, Madison, WI, 53792; Phone: (608) 263-6074; FAX: (608) 263-1466; email: kaufmanp@mhub.ophth.wisc.edu

they exhibited a stable monolayer endothelial-like morphology, and were then treated with H-7 (Sigma Chemical Co., St. Louis, MO) and analyzed.

Image analysis: For time lapse videography, a high resolution black & white charge coupled device (CCD) camera (COHU Inc., Electronics Division, San Diego, CA) was attached to the phototube of a Leitz DMIL inverted phase microscope (Leica, Wetzlar, Germany) and the output was fed to a video recorder and a TV screen. The identical field of cells was recorded at each time interval before and during exposure to H-7 and images were subsequently captured from the videotape. In addition, cells were recorded and then fixed for actin staining as described below after exposure to 20, 100, and 300 μM H-7 for 2 h, as well as after 30 min and 2 h recovery following drug washout. To evaluate the potential toxicity of H-7 for HTM cells, some cells were recorded while exposed to 600 μM H-7 (twice the generally accepted maximal dose for affecting the cytoskeleton in several types of cultured cells [1,7,8], and twice the maximally effective intracameral dose for increasing outflow facility in monkeys [1,9]) for 2 h and during recovery for 30 min and 2 h after drug washout.

Immunocytochemistry: Cells were cultured on glass cover slips pre-coated with poly-L-lysine, incubated with or without H-7 for the indicated time, and then fixed and fluorescently labeled for actin, vinculin, and β-catenin. The cells were washed with 50 mM MES (2-(N-morpholine) ethanesulfonic acid) buffer, and simultaneously permeabilized and fixed with 0.5% Triton X-100 and 3% paraformaldehyde. The cells were then exposed to rhodamine (TRITC) phalloidin (Sigma) for fluorescent labeling of actin, or exposed to monoclonal or polyclonal anti-human vinculin, and β-catenin primary antibodies followed by Texas Red (TR)-conjugated goat anti-mouse second antibody (Jackson Laboratories, West Grove, PA). The cells were examined and images generated using a Zeiss Axiophot fluorescent microscope with a 100x oil immersion lens (Zeiss, Thornwood, NY).

Digital fluorescence microscopy: To quantitatively compare the local labeling intensities of different adhesion molecules including actin, vinculin, paxillin, β-catenin, and phosphotyrosine-containing proteins, digital florescence microscopy was used in separate experiments. Cells were double-labeled for vinculin (cyanine dyes, CY3, Jackson Laboratories) and actin (fluorescein isothiocyanate, FITC, Sigma), paxillin (CY3) and phosphotyrosine (Alexa, Molecular Probes, Inc., Eugene, OR) or β-catenin (CY3) and actin (FITC) respectively. Cells were then washed, fixed and stained as described. Images were acquired using the DeltaVision system (Applied Precision, Issaquah, WA), equipped with a Zeiss Axiovert 100 microscope with a 100x 1.3 NA Plan-Neofluar objective (Oberkochen, Germany) and Photometrics 300 series scientific-grade cooled camera (Tucson, AZ) reading 12 bit images. Images were presented either by true color, or by color spectrum representing fluorescence intensities. FRI between two different components in double-labeled cells was used to determine the dynamics of cellular adherens junctions as described previously [5,10].

RESULTS

HTM cell topography: Untreated HTM cells formed a monolayer of closely attached cells with "endothelial-like" morphology, and remained alike, albeit not identical, in appearance at each time point (Figure 1). Treatment with H-7 induced a dose- and time-dependent cell rounding and apparent thickening toward the center of the cells. A mild effect was observed within 60 min after treatment with 100 μM H-7 and increased with H-7 concentration or exposure time. After exposure to 300 μM H-7 for 1 h, cells became more refractile

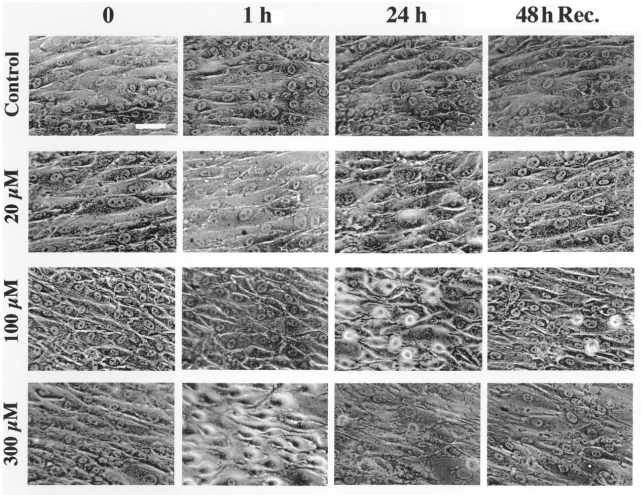

Figure 1. H-7-induced alteration and long-term recovery of cultured HTM cells. Phase contrast videography of cultured HTM cells. Cells were treated with 20, 100, or 300 μM H-7 and recorded at 1, 6, 11 and 24 h, then incubated with H-7-free medium and recorded for another 24 h and 48 h. For each dose, the same field of cells was located and recorded at each time point, and no obvious cell loss was noted. Data for 6 h and 11 h treatment and 24 h recovery are not shown. Bar = 80 μm.

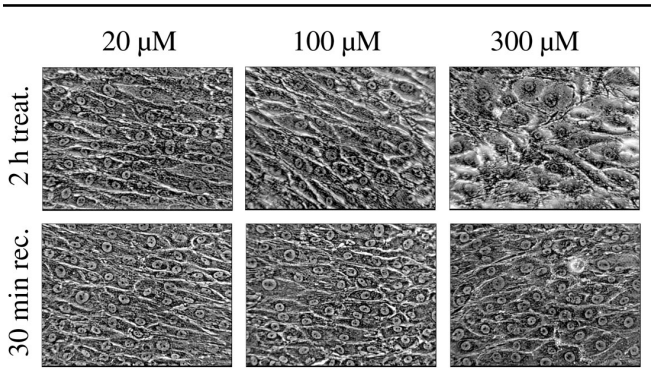

Figure 2. H-7-induced alteration and short-term recovery of cultured HTM cells. Phase contrast videography of cultured HTM cells. Cells were treated with 20, 100, or 300 μM H-7 and recorded at 2 h, then incubated with H-7-free medium and recorded at 30 min and 2 h. For each dose and time point, a different but representative field of cells was recorded, and no obvious cell loss was noted. Data for 2 h recovery are not shown. Bar = 80 μm.

toward the cell center, yet their intercellular contacts were maintained and no cellular separation was observed. After 24 h exposure to H-7, about 50% of the cells treated with 20 μM H-7 appeared to be affected, whereas almost all the cells treated with 100 or 300 μM H-7 were involved (Figure 1). These changes were reversible, and no obviously detached cells were observed at any dose or time of treatment. For the 20 and 100 μM doses (24 h treatment), recovery seemed complete after 48 h in H-7-free medium (Figure 1). Essentially full recovery of the cells after 48 h was also observed for the 300 μM dose, as shown by a typical endothelial morphology. For each dose and time point, a confluent monolayer of cells very similar to the pretreatment appearance was observed and there was no obvious cell loss. This indicates that the cells observed were the original ones, since there was not enough time for new cells to grow to a highly confluent and differentiated appearance. These data suggest that H-7 does not appear to be irreversibly cytotoxic at the highest in vivo intraocular concentration studied [1,9]. Within 30 min after drug removal following 2 h exposure to different doses of H-7, including 600 μM (data not shown), morphological recovery of HTM cells appeared complete (Figure 2). For all doses, 2 h recovery (data not shown) appeared as complete as 30 min recovery, and no obviously detached cells were seen.

Effect of H-7 on the distribution of actin, vinculin, and β-catenin in HTM cells: H-7 induced disruption of the stress fiber network and focal adhesions. Actin-containing bundles deteriorated markedly after 30 min exposure to H-7, especially at the higher doses. With longer exposures (2 h), the stress fiber network was obliterated, especially at higher doses, leaving only a diffuse mesh of actin filaments mostly at the cell periphery (Figure 3). The H-7-treated cells also showed dramatic dose- and time-dependent deterioration of vinculin-containing focal adhesions, with mild alterations in vinculin-containing cell-cell junctions (Figure 4). The distribution of β-catenin was slightly altered, but in general cell-cell junctions were resistant to H-7, especially at lower doses (Figure 5). Staining for β-catenin was weak and cells were occasionally partially separated upon exposure to 300 μM H-7 (Figure 5).

Recovery of the actin-based cytoskeleton and vinculin-containing focal adhesions began as early as 30 min after 2 h treatment with H-7. Actin recovery occurred rapidly in cells treated with any dose, redistributing into both radial and circumferential bundles consistent with the recovery of cell morphology (Figure 2, Figure 3). There was not much difference in β-catenin labeling between H-7 treatment and recovery at the 20 and 100 μM doses; that is, because there was little effect, as described above, there was little recovery to be seen. However, at the 300 μM H-7 dose, which did affect β-catenin, recovery of β-catenin at the cell border was obvious within 30 min after drug removal, exhibiting a continuous zigzag appearance (Figure 5). In contrast, vinculin recovery in cell-matrix and cell-cell adhesions lagged behind that of actin microfilaments (Figure 3, Figure 4).

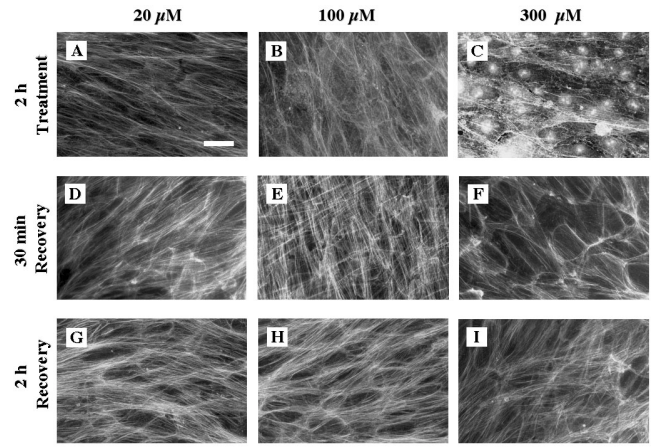

Figure 3. The effects of H-7 on actin microfilaments. Cultured HTM cells were treated with 20, 100, or 300 μM H-7 for 2 h, and then allowed to recover for 30 min or 2 h in H-7-free medium. Bar = 30 μm.

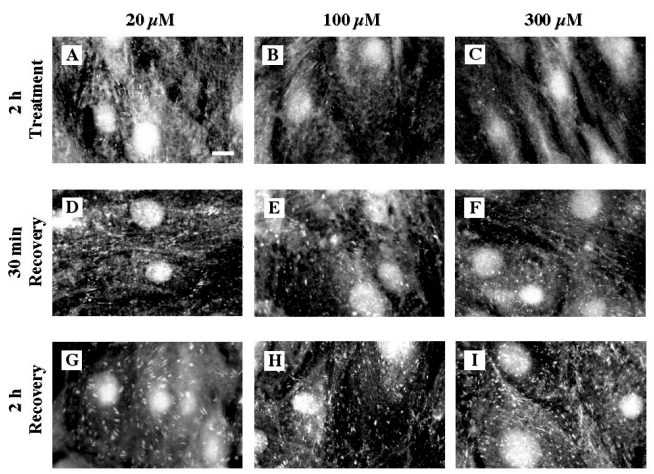

Figure 4. The effects of H-7 on vinculin-containing focal adhesions and cell-cell junctions. Cultured HTM cells were treated with 20, 100, or 300 μM H-7 for 2 h, and then allowed to recover for 30 min or 2 h in H-7-free medium. Bar = 30 μm.

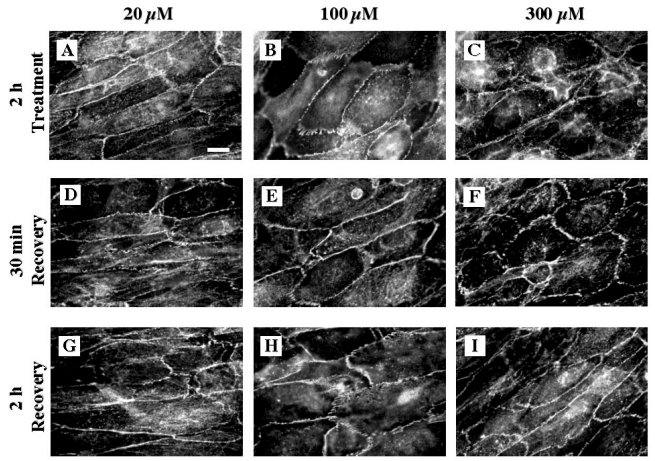

Figure 5. The effects of H-7 on β-catenin. Cultured HTM cells were treated with 20, 100, 300 μM H-7 for 2 h, and then allowed to recover for 30 min or 2 h in H-7-free medium. Bar = 30 μm.

FRI analysis of H-7 induced changes in the actin cytoskeleton and the associated cellular adhesions: As described above, immunofluorescence analysis of HTM cells treated with H-7 demonstrated a striking, dose-dependent, and transient breakdown in the structure and organization of actin, vinculin and, to a limited extend, β-catenin. However, information regarding relative changes and dynamics in the local fluorescence intensities of the molecules associated with cellular adhesions, which is important for understanding the mechanisms underlying the drug's effects, was not defined by the conventional immunocytochemistry. Digital microscopy coupled with FRI analysis of cells double labeled for two proteins was utilized in order to examine the molecular dynamics of these changes in more detail.

Double staining for vinculin (red channel) and actin (green channel) in untreated cells revealed numerous stress fibers oriented primarily parallel to the long axis of the cells, and terminating at vinculin-containing focal adhesions and adherens junctions (Figure 6A-D). FRI analysis (Figure 6D) showed that within most individual adhesions there was extensive overlap between vinculin and actin labeling (i.e., abundance of sites where an intensity ratio of 1:1 was observed). After exposure to 300 μM H-7 for as little as 15 min (Figure 6E-H), HTM cells showed fewer and smaller focal contacts and stress fibers. FRI showed that the actin:vinculin ratio within the vast majority of residual adhesions remained unchanged, indicating a rapid but proportional loss of vinculin and actin from these structures (Figure 6H). This is consistent with the findings at 1 h of exposure to 300 μM H-7, which confirmed a breakdown of both vinculin and actin as well as an unchanged actin:vinculin ratio. Removal of the drug for as little as 5 min resulted in a rapid reorganization of actin filaments and an increase in the size, number, and intensity of vinculin-positive focal adhesions (Figure 6M-P). By 20 min after H-7 removal, actin and vinculin appeared essentially normal (Figure 6Q-T).

Double staining for paxillin (red channel) and phosphotyrosine (green channel) in untreated cells revealed that paxillin, unlike vinculin, was associated only with focal contacts and not with cell-cell junctions. A substantial portion of the phosphotyrosine, but not all, co-localized with paxillin at focal contacts, and was also associated with cell-cell junctions, indicating a positive correlation with cellular adhesions (Figure 7A). HTM cells treated with 300μM H-7 for 15 and 60 min showed a rapid and time-dependent reduction in phosphphotyrosine levels, followed by a slower loss of paxillin,

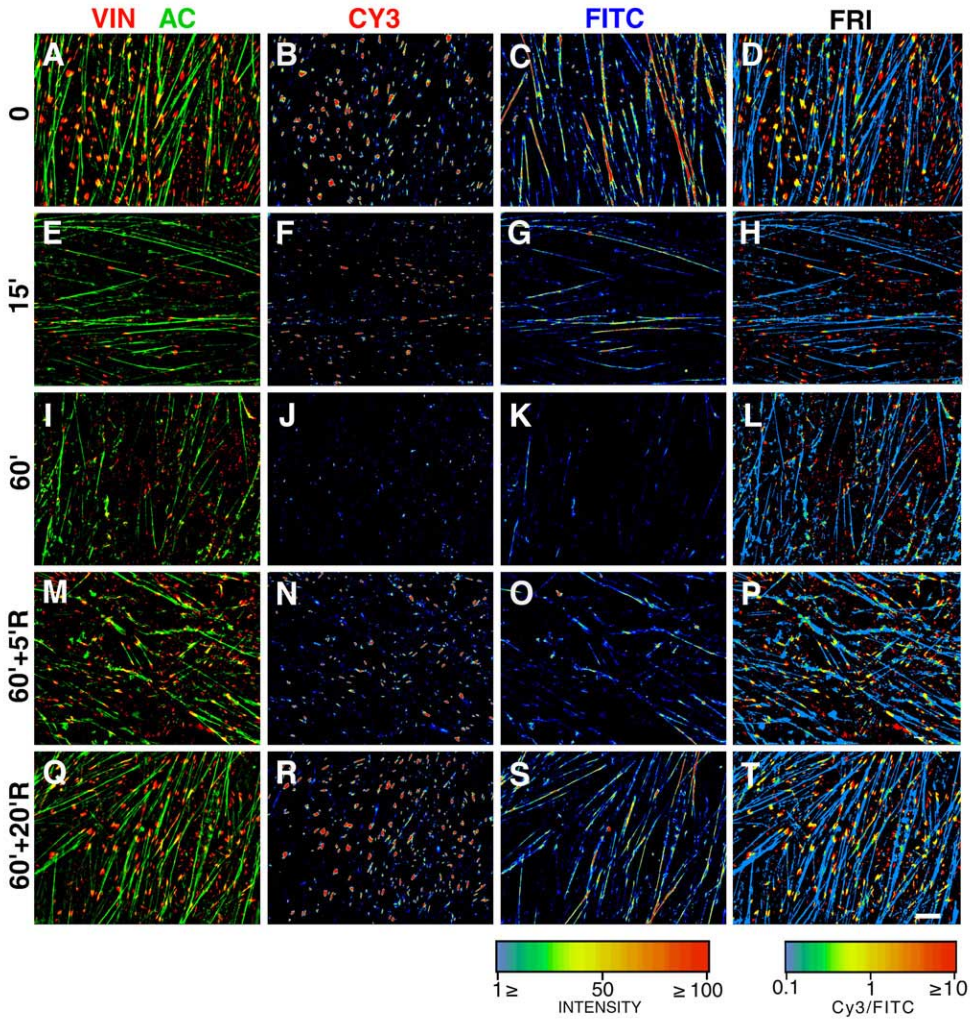

Figure 6. FRI of vinculin and actin in HTM cells treated with H-7. **A**-**L**: Digital microscopic analysis of HTM cells, double-labeled for vinculin (VIN; CY3) and actin (AC; FITC), before (0) and after 15 or 60 min (15'; 60') of treatment with 300 μM H-7. **M**-**T**: Cells treated with H-7 for 1 h and then incubated in medium without H-7 for 5 min or 20 min (60'+5'R; 60'+20'R). The left column shows the superimposed images of vinculin (red) and actin (green). The columns marked CY3 and FITC show the intensity of labeling of the respective proteins, using the spectrum scale presented under the FITC column. The FRI column depicts the CY3-to-FITC intensity ratio (scale shown under the column). Bar = 10 μm.

in focal contacts (Figure 7E-L). FRI again indicated a more significant reduction in the number and intensity of sites positive for phosphphotyrosine than for paxillin and, as a result, a high ratio of paxillin to phosphotyrosine (Figure 7H). The number, size, and labeling intensity of paxillin-positive focal contacts increased dramatically upon removal of H-7 (Figure 7M-T). At 5 min the more prominent focal contacts already contained phosphotyrosine, and their number and size increased with time (Figure 7M-T), but the recovery was not complete, especially for phosphotyrosine, as shown by a fewer number of and less intense labelings, and by the relatively low ratio of the two components, compared to untreated cells (Figure 7Q-T).

Double staining for β-catenin (red channel) and actin (green channel) in untreated cells revealed that intercellular junctions were delineated by β-catenin staining appearing as continuous lines at cell-cell borders. Weaker, but significant actin labeling was also noted along the β-catenin-containing cell-cell adherens junctions, and cell-cell junctions were flanked by prominent actin bundles (Figure 8A-D). Upon H-7 treatment for 15 min, stress fibers and the actin bundles flanking the cell-cell adherens junctions were disrupted, whereas the β-catenin-rich cell-cell adhesions were maintained (Figure 8E-L). FRI analysis showed that the residual actin filaments were not associated with these β-catenin containing adhesions (Figure 8H). By 60 min of H-7 exposure (Figure 8I-L), β-catenin-containing cell-cell junctions were still present but less well organized. FRI indicated that the actin:β-catenin ratio at cell-cell junctions dropped to below 0.1, indicating a relative loss of actin from these structures (Figure 8H). Removal of H-7 resulted in a rapid re-formation of actin filaments and β-catenin-positive structures (Figure 8M-T). Five min after H-7 withdrawal, new stress fibers were formed throughout the ventral aspects of the cells and were also associated with β-catenin-containing cell-cell junctions. By 20 min cell-cell β-catenin-containing adherens junctions flanked by actin bundles were apparent (Figure 8M-T).

DISCUSSION

In this study, the 2-dimensional topographic view of HTM cells showed that H-7-treated cells appeared to round or thicken toward the center in a dose- and time-dependent manner, based on increased refractility of the cells. By inhibiting actomyosin contractility, H-7 secondarily alters actin cytoskeleton orga-

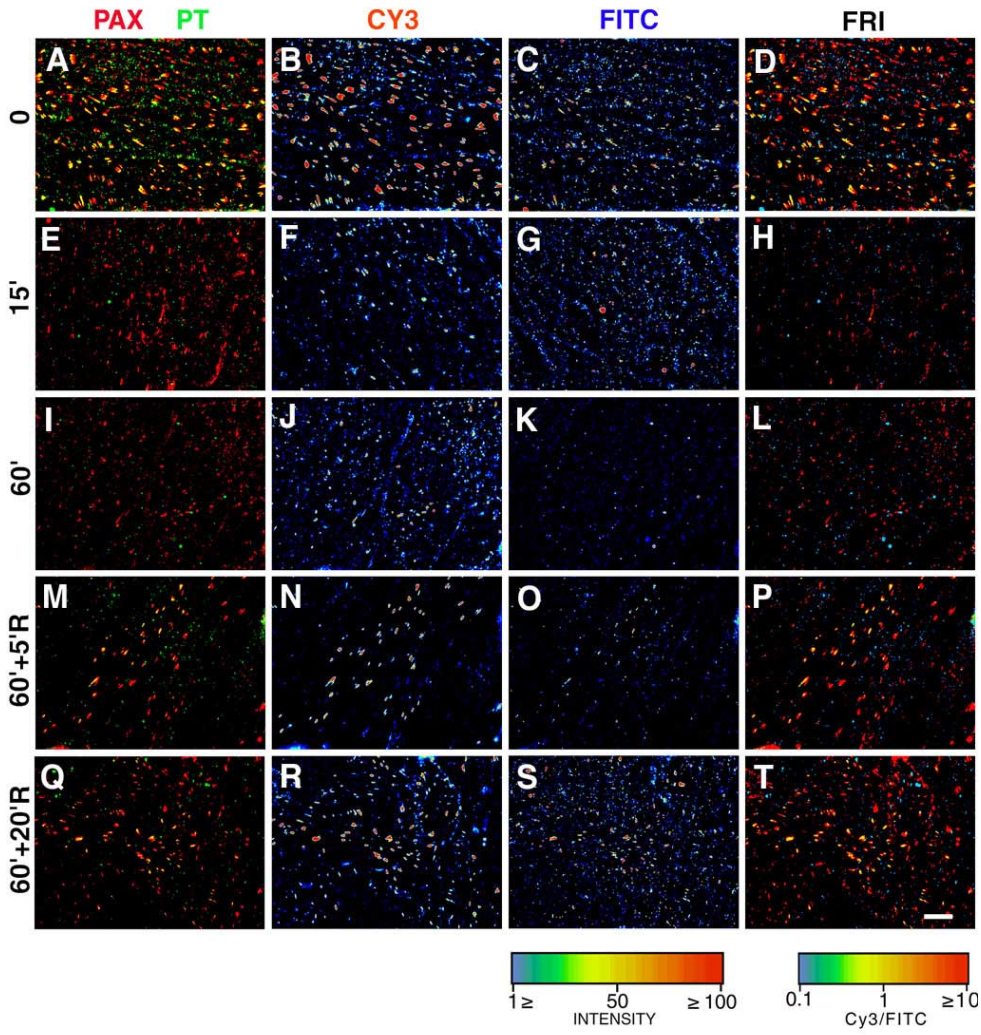

Figure 7. FRI of paxillin and phosphotyrosine in HTM cells treated with H-7. **A-L**: Digital microscopic analysis of HTM cells, double-labeled for paxillin (PAX; CY3) and phosphotyrosine (PT; FITC), before (0) and after 15 and 60 min (15'; 60') of treatment with 300 μM H-7. **M-T**: Cells treated with H-7 for 1 h and then incubated in medium without H-7 for 5 min or 20 min (60'+5'R; 60'+20'R). The left column shows the superimposed images of paxillin (red) and phosphotyrosine (green). The columns marked CY3 and FITC show the intensity of the respective labeling, using the spectrum scale presented under the FITC column. The FRI column depicts the CY3-to-FITC intensity ratio (scale shown under the column). Bar = 10 μm.

nization and the associated focal adhesion complexes [7,11,12], thereby altering cell shape. The changes in cell morphology were consistent with those in the actin cytoskeleton and associated cellular adhesions, indicating that the increased cell refractility appeared subsequent to the H-7-induced disruption of the actin cytoskeleton and cellular adhesions, especially focal adhesions. It was suggested by Bill, Svedbergh, and Mäepea [13,14] that the proper attachment of SC inner wall endothelial cells to the subendothelial tissue is important for the formation of invaginations and pores, the vacuole-like structures in the inner wall cells through which aqueous humor reaches the canal lumen. If the attachment is too strong, the invagination process may not take place; if it is too weak, the inner wall cells might detach [14]. H-7 may loosen focal adhesions but not detach the cells, thus facilitating the formation of invaginations of the inner wall cells and enhancing outflow. Based on H-7's cytoskeletal effects, we may also hypothesize that H-7 can destabilize the overall architecture of the trabecular meshwork by inducing changes in cell shape and cellular attachments, opening the flow pathways and forming new flow routes [9], and thereby reducing flow resistance and IOP [1]. The data suggest that the cytoskeletal system is involved in the normal regulation of aqueous humor outflow resistance and the pathophysiology of certain forms of glaucoma [3,15], and may be targets for H-7 and other compounds capable of increasing outflow facility in vivo. The consistency of our data with studies of H-7-induced changes in outflow facility and TM ultrastructure supports this hypothesis. In monkeys, the maximal H-7-induced IOP reduction occurred at 2 h [1], when considerable disruption of actin and focal contacts was observed in cultured HTM cells. In addition, the H-7-induced outflow facility increase and cellular relaxation in the TM were reversible after the drug was removed from the anterior chamber (AC) for 2.5 h [16], while after 2 h in H-7 free medium, recoveries of actin and associated adhesion molecules of HTM cells were almost complete. However, the cellular mechanisms underlying the outflow increasing effects of various cytoskeletal compounds may not be the same. For example, latrunculin (LAT)-A, which increases facility about as much as H-7, disassembles actin filaments by sequestering monomeric actin, and preferentially affects intercellular adherens junctions [10,17,18]. Cytochalasin B results in an increase in the hydraulic conductivity of cultured monolayers of HTM cells, accompanied by a retraction of the cells and

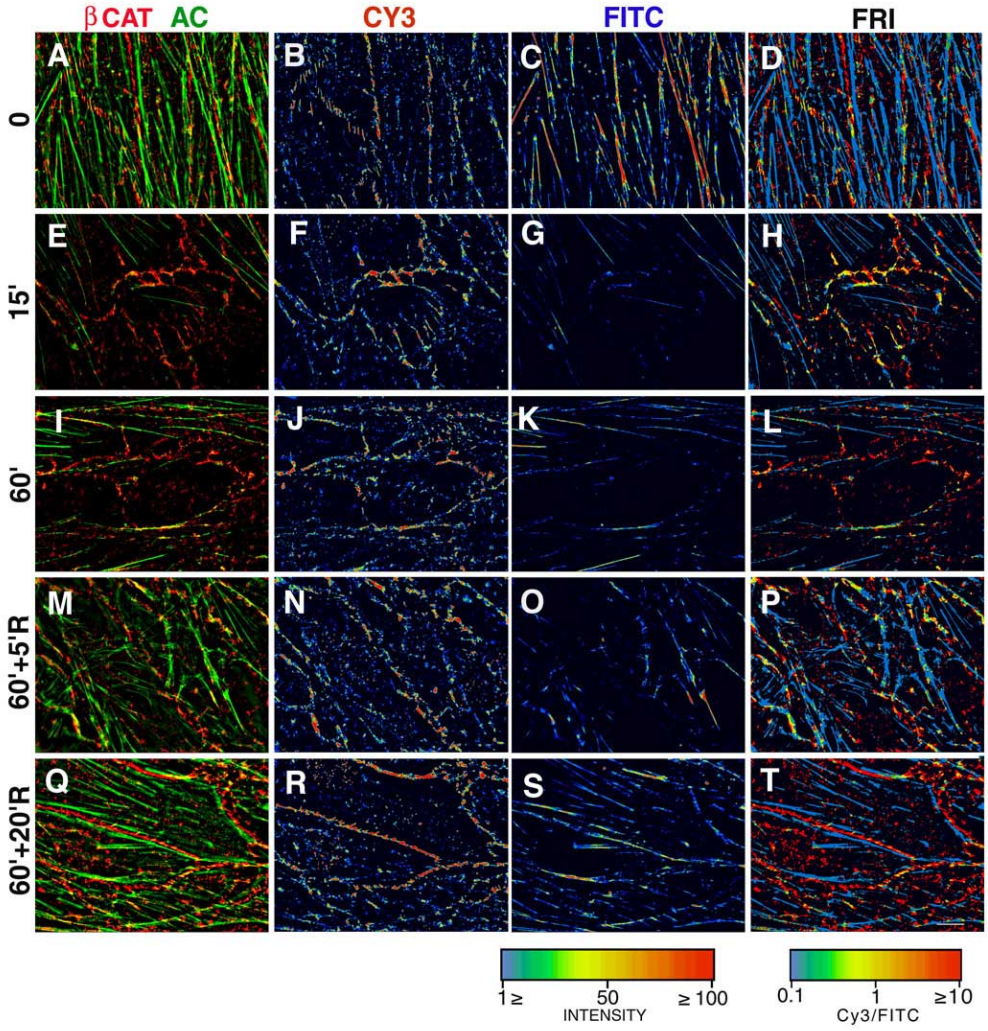

Figure 8. FRI of β-catenin and actin in HTM cells treated with H-7. **A-L**: Digital microscopic analysis of HTM cells, double-labeled for β-catenin (βCAT; CY3) and F-actin (AC; FITC), before (0) and after 15 and 60 min (15'; 60') of treatment with 300 μM H-7. **M-T**: Cells treated with H-7 for 1 h and then incubated in medium without H-7 for 5 min or 20 min (60'+5'R; 60'+20'R). The left column shows the superimposed images of β-catenin (red) and F-actin (green). The columns marked CY3 and FITC show the intensity of labeling of the respective proteins using the spectrum scale presented under the FITC column. The FRI column depicts the CY3-to-FITC intensity ratio (scale shown under the column). Bar = 10 μm.

widening of the intercellular spaces [19], and a disruption of endothelial lining and a washout of extracellular material in TM tissue [20,21]. Calcium chelators, which primarily affect the intercellular junctions, produce a similar cell separation and outflow facility increase in living monkeys [22-24].

The role of intercellular junctions in H-7's ability to enhance outflow across the trabecular meshwork is not clear. Consistent with previous findings [3], our study showed that most cells still remained attached to their neighbors, even at high doses and long duration of H-7 treatment. Studies with other non-ocular cell types [1,7,25] also demonstrated dose- and time-dependent disruption of the actin cytoskeleton and cell-matrix adhesions, with only a relatively modest effect on intercellular junctions following H-7 treatment. Sabanay et al [9] determined the effects of H-7 on TM structure and fluid conductance of live monkeys using colloidal gold as a flow tracer. The data showed that H-7 expanded the intercellular spaces in the juxtacanalicular meshwork accompanied by removal of ECM material, and extended the SC inner wall cells, but had little effect on cell-cell junctions. As a result, gold tracer was widely seen along the inner canal wall but failed to pass between SC cells. It is possible, however, that the intercellular spaces may become slightly "leakier" to aqueous humor but not to gold particles upon H-7 treatment. This hypothesis is consistent with other studies [8,25,26]. In cultured Madin Darby Canine Kidney epithelial cells, H-7 prevented tight junction assembly through its effect on the cytoskeleton, associated with a decrease in transepithelial resistance but without interfering with adherens junction assembly. Taken together, these observations indicate that, as previously proposed [3], even trivial changes in intercellular junctions might also contribute to the effects of H-7 on outflow facility.

In this study, we employed digital microscopy and multiple image processing to characterize the molecular dynamics of various components of the actin cytoskeleton and the associated cellular junctions in cultured HTM cells in response to H-7 treatment. Vinculin-actin FRI revealed largely comparable distribution of the two proteins in focal contacts and in cell-cell junctions. Phosphotyrosine-paxillin FRI pointed to a highly similar labeling (i.e., uniform FRI) of focal contacts, suggesting an active involvement of tyrosine phosphorylation in assembly of focal contacts [5]. β-catenin-actin FRI showed that the cell-cell junctions were flanked by prominent actin bundles as expected from a typical zonula adherens [5]. FRI analysis of the cells at different time points indicated that phosphotyrosine was indeed more sensitive to H-7 than was paxillin. The loss of phosphotyrosine from focal contacts early after addition of H-7 suggests that tyrosine phosphorylation may be preferentially affected as an immediate result of H-7-induced cellular relaxation, leading to the suppression of substrate adhesion formation. However, the dynamics of phosphotyrosine in actin-derived cellular tension as well as intercellular interaction in HTM cells with or without H-7 treatment remains unknown. Clearly more work, including FRI analysis of phosphotyrosine vs. actin and/or intercellular adhesion and other focal adhesion molecules, is needed to elucidate the role of phosphotyrosine in the cellular and molecular basis for the effects of H-7 and other compounds acting via the cytoskeleton on outflow facility.

In previous studies in living monkeys [1], slit lamp examination revealed transient and mild punctate corneal epithelial defects and slight epithelial cloudiness following a topical dose of 150 or 400 mM H-7. The maximal facility-effective dose of topical H-7 (400 mM) also transiently increased the protein concentration in the AC, the rate of entry of i.v. fluorescein into the AC aqueous humor and cornea, and the corneal thickness, and caused the corneal endothelial cell borders to become indistinct on specular microscopy. However, no changes were found in the corneal endothelium and ciliary epithelium by light and electron microscopy, or in the lens and AC by slit lamp biomicroscopy, following a maximal facility-effective dose of intracameral H-7 (300 μM) [1]. This difference is likely due to different drug concentrations in the AC and cornea after different routes of drug administration. The high concentration (400 mM) and small volume (5μl x 4) formulations used in the topical drug protocols place the central cornea, onto which the drops are placed with blinking prevented, at a disadvantage, so that the cornea "sees" a much higher dose with topical than with intracameral administration [27]. Additionally, when penetrating into the cornea after topical administration, H-7 would reach the corneal endothelial cells and their focal contacts from the basement membrane (Descemet's membrane) side. However, when H-7 is delivered intracamerally, the presence of apical tight junctional complexes (maculae occludents) between adjacent cells, may prevent or inhibit the passage of H-7 from the aqueous humor to the lateral and basal aspects of the corneal endothelial cells [28,29].

It is not entirely clear why 300 μM intracameral H-7 induces cytoskeletal changes in the TM/SC but not corneal endothelium and ciliary epithelium. One possible explanation could be that H-7 might affect the TM at lower concentrations than the cornea because of their different tissue architecture and physiologic milieu. The TM is a suspended multilayered tissue, in which juxtacanalicular cells have no real basement membrane and the SC inner wall cells have only a thin, diaphanous, discontinuous basement membrane. When cellular contractility is inhibited by H-7, the TM can be readily distorted and distended by fluid flow down the pressure gradient between the AC and SC. However, the corneal endothelium is a single cell layer on a well-defined basement membrane/ECM structure (Descemet's membrane and stroma) with much less fluid flow across it than the TM and is thus less easily distended or distorted even when the contractile apparatus, and consequently cellular adhesions, are weakened. Similarly, the ciliary body geometry is less likely to be perturbed than the TM. In addition, the juxtacanalicular cells will be continuously bathed on all sides by drug-containing aqueous humor, while the other AC tissues will have at least one aspect facing away from the aqueous. Especially for the posteriorly located ciliary body, the continuous anteriorly directed aqueous flow may result in the ciliary epithelium being exposed to a much lower drug concentration compared to the TM [27].

Nonetheless, potential H-7-induced cytotoxicity is of con-

cern. Our previous and current studies showed that H-7's outflow facility-increasing effect in live monkeys and the effects of H-7 on cell shape, actin cytoskeleton and cellular adhesions were all reversible after drug removal, and no apparent cell death was observed [1]. Particularly, rapid and almost full morphological recovery of HTM cells treated with H-7 occurred even at a 600 µM dose, which is twice the highest in vivo intraocular concentration studied [1]. Those data, plus the absence, or at most, the mild and transitory nature of any ocular side effects following H-7 treatment in vivo, indicate that the reversible changes we observed in cell shape and adhesions induced by H-7 at a 300 µM or lower dose may reflect a pharmacological induction of normal physiologic responses of cells in vivo and in vitro to ambient conditions. Other cytoskeleton-disrupting compounds such as LAT-A and B [17,18] and cytochalasins B and D [30,31] also induce large but reversible increases in outflow facility, again suggesting that the outflow facility increasing effects of such cytoskeletal agents can be relatively gentle and reflect a near-physiological modulation of a basic flow control mechanism rather than irreversible cytotoxicity. Such treatments, if targeted specifically to cells of the outflow pathway, augur well for potential clinical applicability.

ACKNOWLEDGEMENTS

Mary Ann Croft, MS assisted with statistical analysis of cellular topography and Baohe Tian, MD provided valuable editorial contributions. This work was supported by grants EY02698 (PLK), EY02477 (JRP) and EY07336 (CRB) from the National Eye Institute, Bethesda, Maryland; Research to Prevent Blindness, New York, New York (PLK); the Glaucoma Research Foundation, San Francisco, California (PLK and BG); American Health Assistance Foundation (CRB); Yeda Research and Development, the E. Neter Chair in Cell and Tumor Biology, the Minerva Foundation, and the Israel Science Foundation, Rehovot, Israel (BG).

REFERENCES

1. Tian B, Kaufman PL, Volberg T, Gabelt BT, Geiger B. H-7 disrupts the actin cytoskeleton and increases outflow facility. Arch Ophthalmol 1998; 116:633-43.
2. Tian B, Gabelt BT, Peterson JA, Kiland JA, Kaufman PL. H-7 increases trabecular facility and facility after ciliary muscle disinsertion in monkeys. Invest Ophthalmol Vis Sci 1999; 40:239-42.
3. Epstein DL, Rowlette LL, Roberts BC. Acto-myosin drug effects and aqueous outflow function. Invest Ophthalmol Vis Sci 1999; 40:74-81.
4. Gills JP, Roberts BC, Epstein DL. Microtubule disruption leads to cellular contraction in human trabecular meshwork cells. Invest Ophthalmol Vis Sci 1998; 39:653-8.
5. Zamir E, Katz BZ, Aota S, Yamada KM, Geiger B, Kam Z. Molecular diversity of cell-matrix adhesions. J Cell Sci 1999; 112:1655-69.
6. Polansky JR, Wood IS, Maglio MT, Alvarado JA. Trabecular meshwork cell culture in glaucoma research: evaluation of biological activity and structural properties of human trabecular cells in vitro. Ophthalmology 1984; 91:580-95.
7. Volberg T, Geiger B, Citi S, Bershadsky AD. Effect of protein kinase inhibitor H-7 on the contractility, integrity, and membrane anchorage of the microfilament system. Cell Motil Cytoskeleton 1994; 29:321-38.
8. Citi S, Volberg T, Bershadsky AD, Denisenko N, Geiger B. Cytoskeletal involvement in the modulation of cell-cell junctions by the protein kinase inhibitor H-7. J Cell Sci 1994; 107:683-92.
9. Sabanay I, Gabelt BT, Tian B, Kaufman PL, Geiger B. H-7 effects on the structure and fluid conductance of monkey trabecular meshwork. Arch Ophthalmol 2000; 118:955-62.
10. Cai S, Liu X, Glasser A, Volberg T, Filla M, Geiger B, Polansky JR, Kaufman PL. Effect of latrunculin-A on morphology and actin-associated adhesions of cultured human trabecular meshwork cells. Mol Vis 2000; 6:132-43 .
11. Tian B, Millar C, Kaufman PL, Bershadsky A, Becker E, Geiger B. Effects of H-7 on the iris and ciliary muscle in monkeys. Arch Ophthalmol 1998; 116:1070-7.
12. Folsom TD, Sakaguchi DS. Disruption of actin-myosin interactions results in the inhibition of focal adhesion assembly in Xenopus XR1 glial cells. Glia 1999; 26:245-59.
13. Bill A, Svedbergh B. Scanning electron microscopic studies of the trabecular meshwork and the canal of Schlemm—an attempt to localize the main resistance to outflow of aqueous humor in man. Acta Ophthalmol (Copenh) 1972; 50:295-320.
14. Bill A, Mäepea O. Mechanisms and routes of aqueous humor outflow drainage. In: Albert DM, Jakobiec FA, editors. Principles and practice of ophthalmology: basic sciences. Philadelphia: Saunders, 1994. p. 206-26.
15. Epstein DL. Primary open angle glaucoma. In: Epstein DL, Allingham RR, Schuman JS, editors. Chandler and Grant's Glaucoma. 4th ed. Baltimore: Williams & Wilkins; 1997. p. 194-7.
16. Tian B, Gabelt BT, Sabanay I, Geiger B, Kaufman PL. Effect of fluid conductance on reversibility of H-7 effects on outflow facility in monkeys. Invest Ophthalmol Vis Sci 2001; 42:S840.
17. Peterson JA, Tian B, Bershadsky AD, Volberg T, Gangnon RE, Spector I, Geiger B, Kaufman PL. Latrunculin-A increases outflow facility in the monkey. Invest Ophthalmol Vis Sci 1999; 40:931-41.
18. Spector I, Shochet NR, Blasberger D, Kashman Y. Latrunculins—novel marine macrolides that disrupt microfilament organization and affect cell growth: I. Comparison with cytochalasin D. Cell Motil Cytoskeleton 1989; 13:127-44.
19. Perkins TW, Alvarado JA, Polansky JR, Stilwell L, Maglio M, Juster R. Trabecular meshwork cells grown on filters. Conductivity and cytochalasin effects. Invest Ophthalmol Vis Sci 1988; 29:1836-46.
20. Svedbergh B, Lutjen-Drecoll E, Ober M, Kaufman PL. Cytochalasin B-induced structural changes in the anterior ocular segment of the cynomolgus monkey. Invest Ophthalmol Vis Sci 1978; 17:718-34.
21. Johnstone M, Tanner D, Chau B, Kopecky K. Concentration-dependent morphologic effects of cytochalasin B in the aqueous outflow system. Invest Ophthalmol Vis Sci 1980; 19:835-41.
22. Hamanaka T, Bill A. Morphological and functional effects of Na2EDTA on the outflow routes for aqueous humor in monkeys. Exp Eye Res 1987; 44:171-90.
23. Bill A, Lutjen-Drecoll E, Svedbergh B. Effects of intracameral Na2EDTA and EGTA on aqueous outflow routes in the monkey eye. Invest Ophthalmol Vis Sci 1980; 19:492-504.
24. Kaufman PL, Svedbergh B, Lütjen-Drecoll E. Medical trabeculocanalotomy in monkeys with cytochalasin B or EDTA. Ann Ophthalmol 1979; 11:795-6.

25. Citi S. Protein kinase inhibitors prevent junction dissociation induced by low extracellular calcium in MDCK epithelial cells. J Cell Biol 1992; 117:169-78.
26. Denisenko N, Burighel P, Citi S. Different effects of protein kinase inhibitors on the localization of junctional proteins at cell-cell contact sites. J Cell Sci 1994; 107:969-81.
27. Tian B, Sabanay I, Peterson JA, Hubbard WC, Geiger B, Kaufman PL. Acute effects of H-7 on ciliary epithelium and corneal endothelium in monkey eyes. Curr Eye Res 2001; 22:109-20.
28. Hirsch M, Renard G, Faure JP, Pouliquen Y. Study of the ultrastructure of the rabbit corneal endothelium by the freeze-fracture technique: apical and lateral junctions. Exp Eye Res 1977; 25:277-88.
29. Petroll WM, Hsu JK, Bean J, Cavanagh HD, Jester JV. The spatial organization of apical junctional complex-associated proteins in feline and human corneal endothelium. Curr Eye Res 1999; 18:10-9.
30. Kaufman PL, Erickson KA. Cytochalasin B and D dose-outflow facility response relationships in the cynomolgus monkey. Invest Ophthalmol Vis Sci 1982; 23:646-50.
31. Kaufman PL, Barany EH. Cytochalasin B reversibly increases outflow facility in the eye of the cynomolgus monkey. Invest Ophthalmol Vis Sci 1977; 16:47-53.

The print version of this article was created on 2 July 2001. This reflects all typographical corrections and errata to the article through that date. Details of any changes may be found in the online version of the article.